

Relevant energy ranges for astrophysical reaction rates

Thomas Rauscher

Department of Physics, University of Basel, Klingelbergstr. 82, 4056 Basel, Switzerland

Effective energy windows (Gamow windows) of astrophysical reaction rates for (p,γ) , (p,n) , (p,α) , (α,γ) , (α,n) , (α,p) , (n,γ) , (n,p) , and (n,α) on targets with $10 \leq Z \leq 83$ from proton- to neutron-dripline are calculated using theoretical cross sections. It is shown that widely used approximation formulas for the relevant energy ranges are not valid for a large number of reactions relevant to hydrostatic and explosive nucleosynthesis. The influence of the energy dependence of the averaged widths on the location of the Gamow windows is discussed and the results presented in tabular form.

PACS numbers: 98.80.Ft, 26.50.+x, 26.90.+n, 24.60.Dr

I. INTRODUCTION

Astrophysical reaction rates describe the change in abundances of nuclei due to nuclear processes in an astrophysical environment, such as a hot plasma composed of free electrons and atomic nuclei. The reaction rate per particle pair (or reactivity) is found by folding interaction cross sections σ with the appropriate energy distribution of the interacting particles in the plasma. For nucleons and nuclei interacting with each other, the latter is the Maxwell-Boltzmann (MB) distribution, leading to the definition of the reactivity $\mathcal{R} = F\mathcal{I}$ with [1, 2]

$$F = \sqrt{\frac{8}{\pi\mu}} \left(\frac{1}{kT} \right)^{\frac{3}{2}}, \quad (1)$$

$$\mathcal{I} = \int_0^\infty \sigma(E) E e^{-\frac{E}{kT}} dE, \quad (2)$$

where k denotes the Boltzmann constant, T the plasma temperature, and μ the reduced mass $\mu = M_1 M_2 / (M_1 + M_2)$. Although the integration limits run from zero to infinity, the largest contributions to the integral \mathcal{I} stem from a narrowly confined energy range, depending on the energy-dependence of the cross sections and the MB distribution. This relevant energy range has been termed Gamow window for charged particle reactions and is important for both nuclear experimentalists and theoreticians as it defines the energy window within which the reaction cross sections have to be known.

Due to their importance, simple approximation formulas (see Eqs. 7, 8, 12, 13) have been derived to estimate the effective energy windows for reactions (see next sections) and are frequently used. However, the derivation of the formulas makes implicit assumptions which are not always valid and therefore they cannot be applied to a number of important cases. For example, it has been pointed out by [1, 3] that resonances below the conventionally computed Gamow window may contribute significantly to the reaction rate for narrow-resonance capture of charged particles on light targets. It will be shown in the following that this can be understood by a more appropriate treatment of the Gamow window calculation. The applicability of the approximation will be

discussed in more detail and the appropriate energy windows derived quantitatively for charged-particle induced reactions (Sec. II) and for neutral projectiles (Sec. III). Section IV concludes with a discussion of the validity of the present approach and a brief summary.

II. CHARGED-PARTICLE REACTIONS

A. The standard approximation of the Gamow window

The standard approximation of the Gamow window assumes that the energy-dependence of the cross section σ is mainly determined by the projectile's penetration of the Coulomb barrier. The integral \mathcal{I} can then be rewritten as [1, 2]

$$\mathcal{I} = \int_0^\infty S(E) e^{-\frac{E}{kT}} e^{-\frac{b}{\sqrt{E}}} dE, \quad (3)$$

where S is the astrophysical S factor

$$S = \sigma E e^{\frac{b}{\sqrt{E}}} \quad (4)$$

which is assumed to be only weakly dependent on the energy E for non-resonant reactions. The second exponential in Eq. (3) contains the Coulomb penetration through the Sommerfeld parameter $\eta = b/(2\pi\sqrt{E})$ and therefore depends on the charges Z_1 , Z_2 of projectile and target, respectively. While the first exponential decreases with increasing energy, this second one increases, leading to a confined peak of the integrand, the so-called Gamow peak. The location of the peak E_0 is shifted to higher energies with respect to the maximum of the MB distribution at $E_{\text{MB}} = kT$. Assuming a constant S factor, E_0 can be determined analytically to be [1, 2]

$$E_0 = \left(\frac{bkT}{2} \right)^{\frac{2}{3}}. \quad (5)$$

The peak is not symmetrical around E_0 but nevertheless is often approximated by a Gaussian function

$$\mathcal{I}(E) = \mathcal{I}_{\text{max}} e^{-\frac{4(E-E_0)^2}{\Delta^2}}, \quad (6)$$

Table I: Effective energy windows $\tilde{E}_{\text{hi}} - \tilde{\Delta} \leq E \leq \tilde{E}_{\text{hi}}$ for given plasma temperature T . Also given is the energy \tilde{E}_0 of the maximum in the reaction rate integrand and its shift δ relative to the standard formula. The latter is $\delta = \tilde{E}_0 - E_0$ relative to the location of the Gamow peak E_0 for charged-particle induced reactions and $\delta = \tilde{E}_0 - E_{\text{MB}}$ relative to the maximum of the MB distribution at E_{MB} for neutron-induced reactions. This table contains only a few examples. The full table is available at EPAPS [7].

Target	Reaction	T	\tilde{E}_{hi}	$\tilde{\Delta}$	\tilde{E}_0	δ
		[GK]	[MeV]	[MeV]	[MeV]	[MeV]
^{24}Mg	(α, γ)	2.5	2.36	1.05	1.66	-1.16
^{27}Al	(p, γ)	3.5	1.47	1.12	0.65	-0.89
^{40}Ca	(α, γ)	2.0	3.62	1.39	2.85	-0.63
		4.0	4.66	1.97	3.56	-1.97
^{60}Fe	(n, γ)	5.0	1.20	1.20	0.13	-0.30
^{62}Ni	(n, γ)	3.5	1.00	1.00	0.15	-0.15
^{106}Cd	(α, γ)	3.5	10.07	3.44	8.08	-1.17
^{120}Sn	(n, α)	5.0	9.54	4.16	6.92	+6.49
^{144}Sm	(α, γ)	3.5	11.97	3.99	9.90	-1.10
^{169}Tm	(α, γ)	2.0	9.20	2.94	7.61	-0.54
		5.0	13.20	4.27	10.22	-4.79

where $\mathcal{I}_{\text{max}} = \exp(-3E_0/(kT))$ is the maximal value of the product of the two exponentials in Eq. (3) and $\Delta = 4\sqrt{E_0 kT/3}$ is the 1/e width of the peak. Inserting the proper numerical factors and units in Eqs. (5) and (6) leads to the more practical form [1, 2, 4]

$$E_0 = 0.12204 (\mu_A Z_1^2 Z_2^2 T_9^2)^{\frac{1}{3}}, \quad (7)$$

$$\Delta = 0.23682 (\mu_A Z_1^2 Z_2^2 T_9^5)^{\frac{1}{6}}. \quad (8)$$

Here E_0 and Δ are in units of MeV, T_9 is the plasma temperature in GK, and $\mu_A = A_1 A_2 / (A_1 + A_2)$ is the reduced mass number. Equations (7) and (8) are widely used to determine a relevant energy range $E_0 - \Delta/2 \leq E \leq E_0 + \Delta/2$ within which the nuclear cross sections have to be known. This is especially important to guide experiments. For this reason, the standard approximation above is often used by experimentalists.

B. Criticism of the standard approximation

The derivation of Eq. (5) – and hence of Eqs. (7), (8) – implicitly assumes that the energy-dependence of the cross section σ is dominated by the Coulomb barrier penetration of the projectile. In other words, the energy-dependence of the entrance channel width dominates. Resonant cross sections can be written as sum of Breit-Wigner terms. It can be shown [5] that for a sufficiently high nuclear level density at the compound nucleus formation energy the sum of overlapping resonances can be replaced by a sum over averaged widths (or averaged

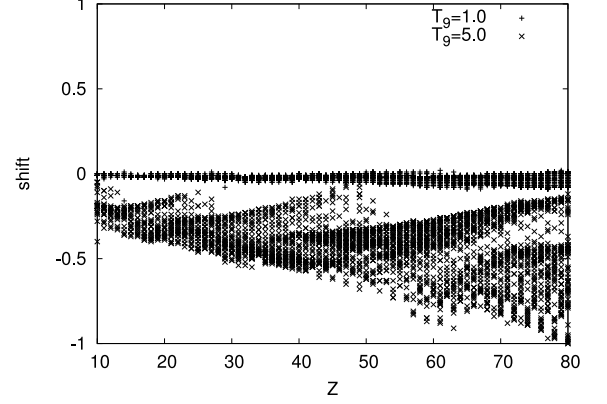


Figure 1: Shifts δ of the maximum of the integrand relative to E_0 of the Gaussian approximation as function of the target charge Z for (p,n) reactions at two temperatures. Almost no shift is observed at $T_9 = 1.0$ and shifts remain small for $T_9 = 5.0$.

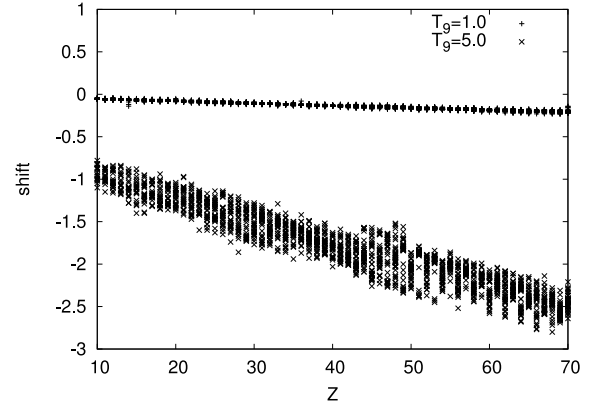


Figure 2: Shifts δ of the maximum of the integrand relative to E_0 of the Gaussian approximation as function of the target charge Z for (α, n) reactions at two temperatures. Almost no shift is observed at $T_9 = 1.0$ and shifts reach a few MeV for $T_9 = 5.0$.

strength functions), leading to the well-established statistical model of compound reactions (Hauser-Feshbach model). Thus, both resonant and Hauser-Feshbach cross sections can be expressed as [5]

$$\sigma \propto \sum_n (2J_n + 1) \frac{X_{\text{in}}^{J_n} X_{\text{fi}}^{J_n}}{X_{\text{tot}}^{J_n}}, \quad (9)$$

with X being either Breit-Wigner widths or averaged Hauser-Feshbach widths, depending on the context. The width of the entrance channel is given by $X_{\text{in}}^{J_n}$, the one of the exit channel by $X_{\text{fi}}^{J_n}$, and the total width including

all possible emission channels from a given resonance or compound state with spin J_n by $X_{\text{tot}}^{J_n} = X_{\text{in}}^{J_n} + X_{\text{fi}}^{J_n} + \dots$. Even in the case of the statistical model only few summands in Eq. (9) contribute although the sum runs over all values of J .

It has become common knowledge that a cross section of the form shown in Eq. (9) is determined by the properties of the smaller width in the numerator if no other channels than the entrance and exit channel contribute significantly to $X_{\text{tot}}^{J_n}$. Then $X_{\text{tot}}^{J_n}$ cancels with the larger width in the numerator and the smaller width remains. (The effect is less pronounced and requires more detailed investigation when other channels are non-negligible in $X_{\text{tot}}^{J_n}$.) In consequence, the energy-dependence of the cross section will then be governed by the energy dependence of this smallest X^J . Only if this happens to be a charged-particle (averaged) width in the entrance channel, the use of the standard formula for the Gamow window (Eqs. 7, 8) will be justified. Since X_{in}^J and X_{fi}^J have different energy dependences, it will depend on the specific energy (weighted by the MB distribution) which of the widths is smaller. Higher plasma temperature will select an energy range at higher energy. Therefore, the relative sizes of the X^J and thus the energy dependence of the cross sections in the relevant energy range will depend on the plasma temperature. This determines the Gamow windows.

It can be seen immediately that the prerequisite for applying the standard formula may not be met when studying reactions like (p, α) at moderate reaction Q values where one would expect the α width to be smaller than the proton width. Also for charged particle capture the standard formula will be problematic as long as the γ width is smaller than the width in the entrance channel. Although astrophysically relevant interaction energies are so small that charged particle widths often become smaller than the radiation widths due to the Coulomb barrier, reactions in high temperature environments – such as explosive nucleosynthesis – may still exhibit the opposite relation. Because of the sensitivity of the Gamow window to the relative sizes of the widths and the complicated dependence of the widths on the interaction energy, Gamow windows should be extracted from numerical inspection of the integrand in Eq. (2) and not from the standard formula which is only applicable for a limited number of cases. This was performed in this work as described in the following sections.

C. Numerical calculation of Gamow windows

The function

$$\mathcal{F}(E) = \sigma(E) E e^{-\frac{E}{kT}} \quad (10)$$

was computed for all targets and reactions given in [6]. The energies of the maxima \tilde{E}_0 and the widths $\tilde{\Delta}$ of the peaks of \mathcal{F} were determined for each case. A full table of the results is available as a machine-readable file from

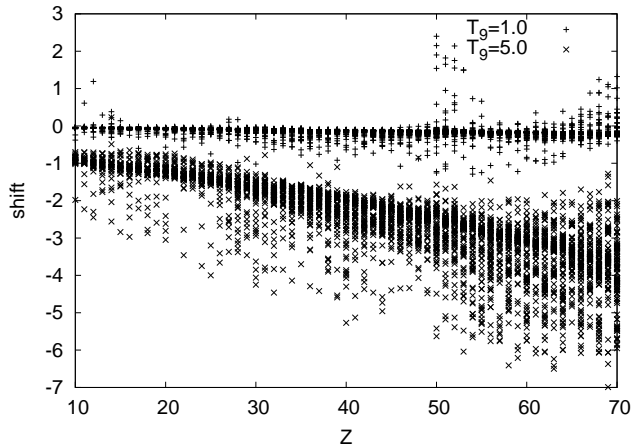


Figure 3: Shifts δ of the maximum of the integrand relative to E_0 of the Gaussian approximation as function of the target charge Z for (α, γ) reactions at two temperatures. Almost no shift is observed at $T_9 = 1.0$ but shifts become large at $T_9 = 5.0$.

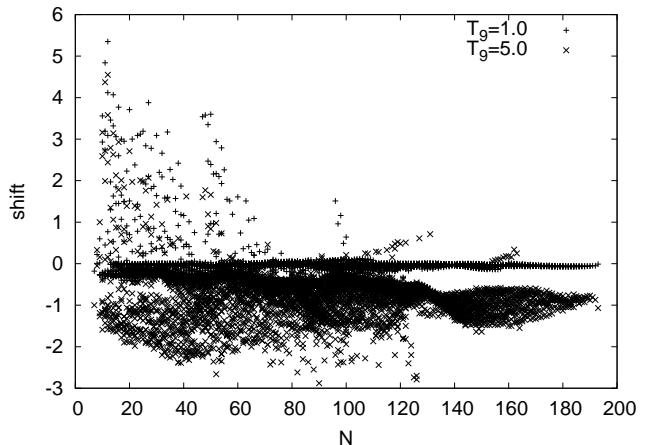


Figure 4: Shifts δ of the maximum of the integrand relative to E_0 of the Gaussian approximation as function of the target neutron number N for (p, γ) reactions at two temperatures. Almost no shift is observed at $T_9 = 1.0$, except for proton-rich nuclei with negative reaction Q value. Shifts remain smaller than for (α, γ) at $T_9 = 5.0$.

EPAPS [7] or at the author's website [8]. With the exception of captures, only reactions with positive reaction Q value are shown. This is the preferred reaction direction to be investigated to minimize stellar plasma effects due to thermal population of the target states [9, 10]. The effective energy window of the reverse reaction can be found by shifting the energy window by the Q value. For captures also reactions with $Q < 0$ are shown, similar to what is given in [6]. Table I, shown here, is only an abbreviated table to illustrate the kind of information contained in the full table for a few selected examples. The full table contains the Gamow windows of 20540 charged-particle reactions for temperatures $0.5 \leq T \leq 5.0$ GK,

involving targets from proton- to neutron-dripline and with charge numbers $10 \leq Z \leq 83$.

It has to be noted that the definition of the width $\tilde{\Delta}$ of the “true” Gamow window used here differs from the definition of the width Δ as used in Eq. (8). The width from the standard approximation is the $1/e$ width of the Gaussian function. However, caution is advised whenever using the energy range defined in such a manner for, e.g., deriving the energies at which experimental cross sections are to be determined. For the numerically derived “true” Gamow windows of this work I found that the area of the peak limited by the $1/e$ width contains only 55 – 70% of the total contribution to the integral, which would lead to a similar uncertainty in the reaction rate even when the cross sections within the window were experimentally completely determined. To obtain a better measure for the relevant energy range, for each case (of given reaction on specific target at given temperature) an energy range was numerically determined contributing 90% of the total integral of Eq. (2). This is the width $\tilde{\Delta}$ quoted in Table I and in the EPAPS table [7].

The energy of the maximum at \tilde{E}_0 determines where the cross sections have the largest weight in the integral. In most cases, however, the relevant energy window is not symmetric around this energy. For a more accurate specification of the energy window, I also give the energy \tilde{E}_{hi} of the upper end of the window in the tables. Thus, the range of relevant energies is defined as

$$\tilde{E}_{hi} - \tilde{\Delta} \leq E \leq \tilde{E}_{hi} \quad (11)$$

In the following I present general observations and discuss selected cases of interest. In general, the shifts $|\delta|$ will be larger, the higher the temperature. Also, the shifts will be larger with higher charge of the involved particle. These main effects are moderated, however, by the involved interplay of different Coulomb barriers in different channels and different reaction Q values leading to a more complicated energy dependence of the widths and thus also of the cross sections.

Since neutrons do not experience a Coulomb barrier and neutron widths are larger than charged particle widths at low energies in most cases, the charge and temperature effects can be seen clearest in (p,n) and (α ,n) reactions, shown in Figs. 1 and 2. In both types of reactions there are no or only small shifts at $T_9 = 1.0$ but large shifts at $T_9 = 5.0$. The magnitude of the shifts is generally larger for the (α ,n) reactions (note the different scale of the figures) due to the higher charge of the α particle. The $|\delta|$ also increase with increasing target charge Z in both cases. The shifts are always to smaller energy because the energy dependence of the neutron widths selects an effective energy close to E_{MB} (see Sec. III) which is always below E_0 .

Charged-particle capture is important in a variety of astrophysical processes. As mentioned in Sec. II B, for capture reactions the applicability of the standard approximation depends on the size of the γ width X_γ^J rel-

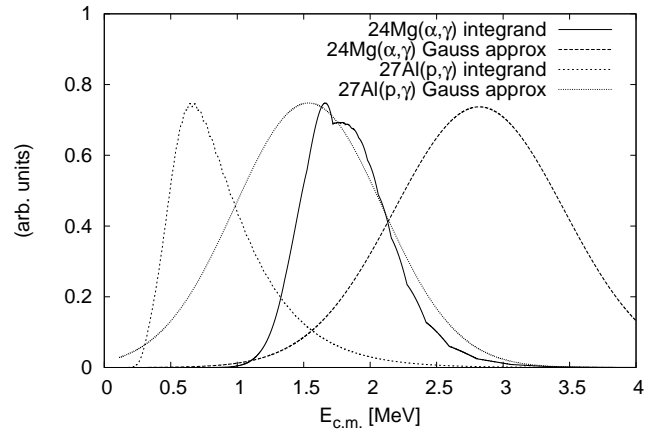


Figure 5: Comparison of actual reaction rate integrand \mathcal{F} and Gaussian approximation of the Gamow window for the reactions $^{24}\text{Mg}(\alpha,\gamma)^{28}\text{Si}$ at $T = 2.5$ GK and $^{27}\text{Al}(p,\gamma)^{28}\text{Si}$ at $T = 3.5$ GK. The integrands and the Gaussians have been arbitrarily scaled to yield similar maximal values.

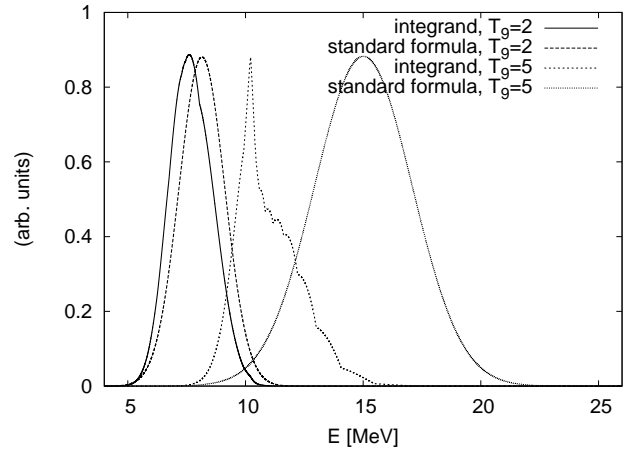


Figure 6: Comparison of actual reaction rate integrands \mathcal{F} and Gaussian approximations of the Gamow window for the reaction $^{169}\text{Tm}(\alpha,\gamma)^{173}\text{Lu}$ at $T = 2$ and 5 GK. The integrands and the Gaussians have been arbitrarily scaled to yield similar maximal values. While the shift is small for $T_9 = 2$, it is about 5 MeV at $T_9 = 5$. Also the asymmetry of the integrand can be clearly seen at $T_9 = 5$.

ative to the projectile width X_{in}^J . When $X_\gamma^J \ll X_{in}^J$, one would assume that there is no Gamow window as the energy dependence of the γ width does not show the strong increase with increasing energy as a charged-particle width [1]. However, effectively the Gamow window is shifted only to much lower energy. This can be understood by the fact that the integration limit in Eq. (2) starts at zero energy and thus will always either include a region where $X_{in}^J \ll X_\gamma^J$ and the Coulomb penetration is competing with the decay of the MB distribution at larger energies, or the low-energy region of the MB distribution suppressing a weakly energy-dependent radiation width. Both cases lead to a peak in the inte-

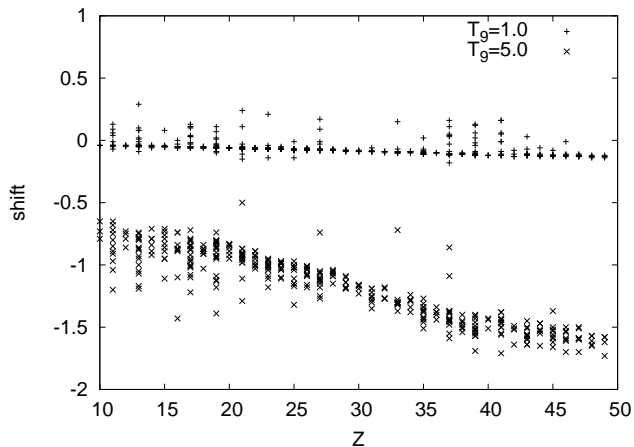


Figure 7: Shifts δ of the maximum of the integrand relative to E_0 of the Gaussian approximation as function of the target charge Z for (α, p) reactions at two temperatures. Almost no shift is observed at $T_9 = 1.0$ and shifts reach a few MeV for $T_9 = 5.0$.

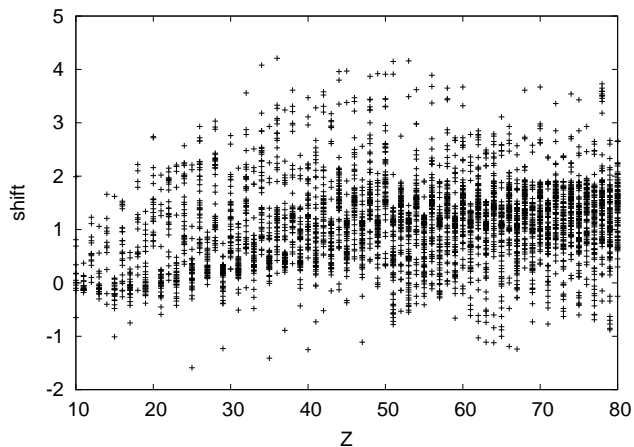


Figure 8: Shifts δ of the maximum of the integrand relative to E_0 of the Gaussian approximation as function of the target charge Z for (p, α) reactions at $T = 5$ GK. The shifts are larger as for (α, p) reactions and they are positive.

grand \mathcal{F} although the “peak” may be located so that it closely approaches zero energy. Figure 3 shows a similar temperature dependence of the shifts for α captures as for (α, n) , although the magnitude of the shifts is larger. These shifts are caused by the fact that at higher T energy regions with $X_\alpha^J \gg X_\gamma^J$ receive a larger weight by the MB distribution. Positive shifts appear for cases with $Q < 0$, simply because the Gamow energy E_0 derived from Eq. (7) is below the (α, γ) threshold and the actual energy window opens at higher energy. The situation is similar for (p, γ) reactions but the temperature dependence is not as pronounced. The positive shifts occur for proton-rich targets at the proton dripline, as can be seen in Fig. 4, plotting the shifts versus the neutron number N .

The astrophysical importance of capture reactions warrants to study a few cases in more detail. As already pointed out in [1, 3], it was experimentally found that also resonances below the Gamow window, as defined by the standard approximation formula, significantly contribute to the reaction rate for certain capture reactions, e.g., $^{24}\text{Mg}(\alpha, \gamma)^{28}\text{Si}$ and $^{27}\text{Al}(p, \gamma)^{28}\text{Si}$. The results for these reactions are given in Table I. Figure 5 shows a comparison of the actual integrands \mathcal{F} and the Gaussian functions obtained by application of Eqs. (7), (8). This can directly be compared to figure 3.24 of [1] where the relative contributions of resonances are compared to the Gamow window derived from the standard approximation (for a brief discussion of the relevance of the Gamow window for narrow resonances, see Sec. IV). The present results show that the approximation is not valid and the actual Gamow window is shifted to lower energy in agreement with what was found in [1] but quantifying the relevant energy window. A similar case is $^{40}\text{Ca}(\alpha, \gamma)^{44}\text{Ti}$, where the effective energy window is also considerably shifted to lower energy. A plot comparing the actual integrand of the reaction rate with the Gaussian approximation can be found in [11]. A further example is the reaction $^{169}\text{Tm}(\alpha, \gamma)^{173}\text{Lu}$, shown in Fig. 6. Again, the shift is considerable at a temperature reached in explosive nucleosynthesis. It is larger than the shifts for lighter targets because of the larger Coulomb barrier. The increasing asymmetry of the peak with increasing temperature can also nicely be seen.

Finally, we might expect that reactions with charged particles in both channels show the most complicated dependence on temperature and charge. However, it is found that the obtained shifts are negligible at low temperature, which can be explained by the fact that the energy dependence of the entrance width dominates at low interaction energies. Figure 7 shows that at $T_9 = 5$ similar values of the shifts are obtained in (α, p) reactions as in (α, n) reactions, smaller than for (α, γ) . The shifts are also negligible at low temperature for (p, α) reactions but larger and *positive* ($\delta > 0$) shifts are found at high temperature (see Fig. 8). This is because the proton widths quickly become larger than the α widths at higher energies and this leads to a dominance of the α width energy dependence. Due to the higher Coulomb barrier, the effective energy window is then found at higher energy as compared to the Gamow window calculated for protons. This effect is shown in more detail in Fig. 9 for $^{112}\text{Sn}(p, \alpha)^{109}\text{In}$ at $T_9 = 5.0$.

III. REACTIONS WITH NEUTRONS

Neutrons are not subject to a Coulomb barrier and therefore a Gamow peak cannot be defined as in Eq. (3). Nevertheless, an effective energy range can be found because $\sigma(E)$ usually is a slowly varying function which can be parameterized depending on the dominant partial wave, i.e., $\sigma \propto 1/\sqrt{E}$ for s-waves, $\sigma \propto \sqrt{E}$ for p-waves,

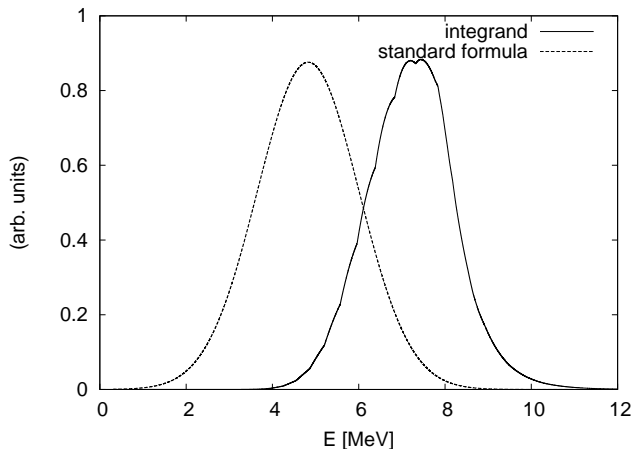


Figure 9: Comparison of the actual reaction rate integrand \mathcal{F} and the Gaussian approximation of the Gamow window for the reaction $^{112}\text{Sn}(p,\alpha)^{109}\text{In}$ at $T = 5$ GK. The two curves have been arbitrarily scaled to yield similar maximal values. The maximum of the integrand is shifted by several MeV to energies higher than the maximum E_0 of the Gaussian.

and $\sigma \propto E^{3/2}$ for d-waves. Then the integrand \mathcal{F} defined in Eq. (2) will exhibit a peak mainly determined by the peak of the MB distribution $E_{\text{MB}} = kT$, only slightly shifted for partial waves $\ell > 0$ due to the angular momentum barrier. An often used approximation is [4, 12]

$$E_{\text{eff}} \approx 0.172T_9 \left(\ell + \frac{1}{2} \right), \quad (12)$$

$$\Delta_{\text{eff}} \approx 0.194T_9 \sqrt{\ell + \frac{1}{2}}, \quad (13)$$

giving the effective energy window $E_{\text{eff}} \pm \Delta_{\text{eff}}/2$ in MeV for neutrons with energies less than the centrifugal barrier. This expression is not as handy as the one for the charged-particle Gamow peak because the dominant partial wave is not known a priori. Nevertheless, the shifts with partial wave are comparatively small and the assumption of s-waves is sufficient to define a useful energy window.

A straightforward application of Eqs. (12), (13) will not be valid in all cases. Just as it was the case with the approximation for charged projectiles in Sec. II, the derivation of the formula implicitly assumes that the energy dependence of the cross section is determined by the neutron projectile. This is justified for low-energy direct capture or reactions through wings of broad resonances. In the general resonant case (and the case of averaging over a large number of resonances as performed in statistical model calculations), however, the energy dependence of the exit channel width can become important and strongly modify the effective energy window.

Similar to the reactions with charged projectiles discussed in Sec. II, the actual effective energy windows were derived by calculating $\mathcal{F}(E)$ from Eq. (10) and numerically determining its maximum and the range of the

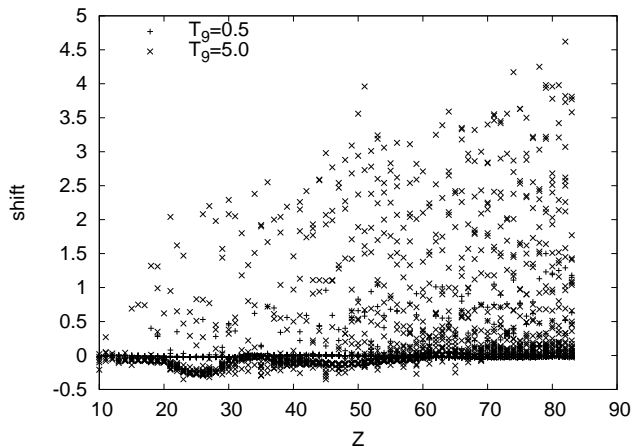


Figure 10: Shifts δ of the maximum of the integrand relative to E_{MB} as function of the target charge Z for (n,p) reactions at two temperatures. Almost no shift is observed at $T_9 = 0.5$ but shifts become large at $T_9 = 5.0$.

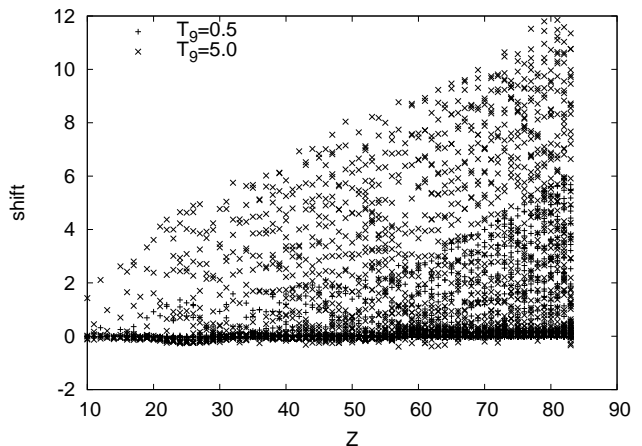


Figure 11: Shifts δ of the maximum of the integrand relative to E_{MB} as function of the target charge Z for (n,p) reactions at two temperatures. Almost no shift is observed at $T_9 = 0.5$ but shifts become very large at $T_9 = 5.0$.

main contributions to the rate integral (Eq. 2). Neutron capture as well as (n,p) and (n,α) reactions are also included in the EPAPS table [7]. Just as for charged particle reactions only reactions with positive Q value are listed, except for (n,γ) reactions which also include a number of endothermic neutron captures at the dripline. This amounts to a total of 8862 neutron-induced reactions. Table I shows a few selected examples. The shifts δ given for neutron-induced reactions are relative to the peak of the MB distribution as this defines the location of the peak for neutron s-waves: $\delta = \bar{E}_0 - E_{\text{MB}}$. The effective energy window is again given by Eq. (11).

The shifts are zero or small for most neutron captures, except for those close to the neutron dripline. One would assume that this confirms the validity of Eqs. (12), (13) for (n,γ) reactions. However, it is rather due to the fact

that the total γ widths, being smaller than the neutron widths in Eq. (9), have a comparatively weak energy dependence and do not move the maximum of the integrand \mathcal{F} from the one given by the MB distribution. This explains why all of the maxima \tilde{E}_0 are more or less identical to E_{MB} and thus also $\tilde{E}_0 \approx E_{\text{eff}}$, with the E_{eff} for $\ell = 0$. A different behavior is only found at low neutron separation energies where either γ widths show a stronger energy dependence or neutron widths become the smallest widths in the reaction channels. Only in the latter case different neutron partial waves will be important in Eq. (12).

Despite of the small absolute shifts for neutron captures, it becomes apparent that the relevant energy window as defined by Eq. (11) reaches down to the reaction threshold if one desires to determine the reaction rate with high integration accuracy, even at high plasma temperature (see also the examples in Table I).

Larger shifts are found for reactions with charged particles in the exit channel. Contrary to most cases discussed in Sec. II, the shifts are positive for the majority of the neutron-induced reactions because the Coulomb barrier penetration in the exit channel moves the energy window to higher energy. As expected, the shifts are larger for increased temperature, increased charge of the compound nucleus, and increased charge of the ejectile. Figures 10 and 11 illustrate these dependences for (n,p) and (n, α) reactions. For $T_9 = 0.5$ the shifts are close to zero whereas they can reach several MeV at $T_9 = 5$. The behavior within an isotopic chain is shown in Fig. 12 for (n, α) on Sn isotopes. Again, for low temperature the effective energy window is barely shifted from the one predicted by the standard formula. With increasing temperature the shift becomes larger. The shifts for the neutron-rich nuclei are larger as the energy dependence of the α width becomes stronger with decreasing Q value.

IV. CONCLUDING DISCUSSION

It has to be pointed out that the preceding discussion made implicit assumptions which have to be scrutinized in any application of the results. An obvious assumption is that the used cross sections are correct. The results should be quite robust because the gross energy dependence of the cross section is the relevant quantity and not its absolute value. The results shown here were obtained with the set 'FRDM' given in [6]. The energy dependence of the particle widths is also sensitive to the Q value and low-lying nuclear states which can be populated in the reaction. Accordingly, updates in masses and spins may affect the conclusions. However, a large change in the derived energy windows is not to be expected because most of them are determined by the Coulomb barrier penetration.

Another source of concern may be the use of statistical model Hauser-Feshbach cross sections for nuclei with low level density close to the driplines, especially for rates

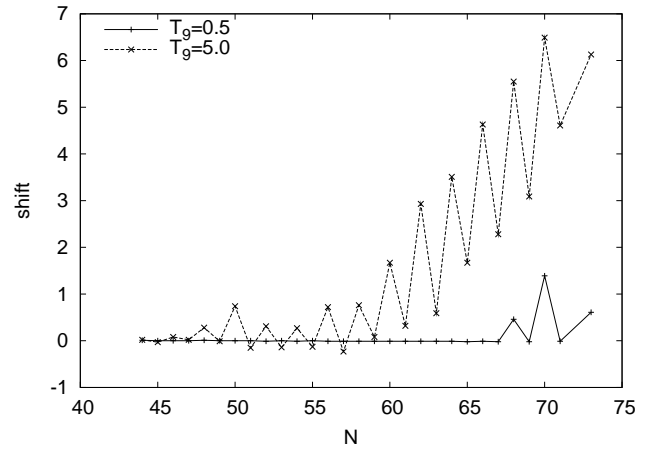


Figure 12: Shifts δ of the maximum of the integrand relative to E_{MB} as function of the target neutron number N for (n, α) reactions on Sn isotopes at two temperatures. Almost no shift is observed at $T_9 = 0.5$ but shifts become large at $T_9 = 5.0$ for the neutron-rich isotopes with small reaction Q value.

at low plasma temperature. As explained below, the derived effective energy windows remain valid even when single resonances contribute and therefore this is not a limitation of the method.

A final assumption seems to be that the cross sections are smooth without isolated resonance features. The notion of a single Gamow peak loses its validity when small, isolated resonances are dominating the reaction rate. In this case, the Gamow window would be fragmented into several Gamow peaks of different importance, depending on the resonance strengths. It can be shown, nevertheless, that the notion of an effective energy window remains valid and that only resonances within the energy window contribute significantly to the reaction rate (for details see [1]). This applies provided the energy windows are derived as shown above. It does not make a statement about the relative importance of resonances because this depends on the actual resonance strengths, not just on the energy dependence of the widths.

Summarizing, a complete numerical study of the effective energy windows for nuclear reaction rates has been performed for reactions induced by nucleons and α particles. It has been shown that the actual energy range of relevant cross sections differs considerably from the ranges obtained by application of the standard formulas. The origin of this difference was explained and extensive tables of the actual energy windows were given. This will be important for further theoretical improvements of reaction rates as well as for helping to design experiments to measure cross sections at energies of astrophysical importance.

Acknowledgments

This work was supported by the Swiss NSF, grant 200020-122287.

-
- [1] C. Iliadis, *Nuclear Physics of Stars* (Wiley VCH, 2007).
 - [2] C. S. Rolfs and W. S. Rodney, *Cauldrons in the Cosmos* (University of Chicago Press, 1986).
 - [3] J. R. Newton, C. Iliadis, A. E. Champagne, A. Coc, Y. Parpottas, and C. Ugalde, *Phys. Rev. C* **75**, 045801 (2007).
 - [4] T. Rauscher, F.-K. Thielemann, and K.-L. Kratz, *Phys. Rev. C* **56**, 1613 (1997).
 - [5] P. Descouvemont and T. Rauscher, *Nucl. Phys. A* **777**, 137 (2006).
 - [6] T. Rauscher and F.-K. Thielemann, *Atomic Data Nucl. Data Tables* **79**, 47 (2001).
 - [7] See EPAPS Document No. [number will be inserted by publisher] at [URL] for a ASCII file containing the full table of energy windows and shifts. For more information on EPAPS, see <http://www.aip.org/pubservs/epaps.html>.
 - [8] <http://nucastro.org>
 - [9] G. G. Kiss, T. Rauscher, Gy. Gyürky, A. Simon, Zs. Fülöp, and E. Somorjai, *Phys. Rev. Lett.* **101**, 191101 (2008).
 - [10] T. Rauscher, G. G. Kiss, Gy. Gyürky, A. Simon, Zs. Fülöp, and E. Somorjai, *Phys. Rev. C* **80** 035801 (2009).
 - [11] R. D. Hoffman, *et al.*, *Astrophys. J.*, in press; arXiv:1003.0110.
 - [12] R. V. Wagoner, *Astrophys. J. Suppl.* **18**, 247 (1969).